

EE

# Rebound Coefficient of Collisionless Gas in a Rigid Vessel : a Model of Reflection of Field-Reversed Configuration

Yuichi Takaku\* and Shigeo Hamada†

Department of Physics, College of Science and Technology,  
Nihon University,  
Kanda-Surugadai Chiyoda-ku, Tokyo 101



## Abstract

A system of collisionless neutral gas contained in a rigid vessel is considered as a simple model of field-reversed configuration (FRC) plasma reflected by a magnetic mirror. The rebound coefficient of the system is calculated as a function of the incident speed of the vessel normalized by the thermal velocity of the gas before reflection. The coefficient is compared with experimental data of FIX (Osaka U.) and FRX-C/T (Los Alamos N.L.). Agreement is good for this simple model. Interesting is that the rebound coefficient takes the smallest value ( $\sim 0.365$ ) as the incident speed tends to zero and approaches unity as it tends to infinity. This behavior is reverse to the one expected for the system with collision dominated fluid instead of collisionless gas. So, by examining the rebound coefficient, it can be successfully inferred whether the ion mean free path in FRC plasma is longer or shorter than the plasma length.

## Keywords

plasma, nuclear fusion, field-reversed configuration,  
rebound coefficient, rarefied gas

## 1 Introduction

There have been many experiments of translation<sup>[1~8]</sup> of field-reversed configuration (FRC) plasmas<sup>[9]</sup>. Motivations of these experiments are briefly reviewed in ref.9: adiabatic compression heating, preventing decay of external magnetic field, diagnostics, fuelling by pellet injection and for FRC reactor studies. As for the last one, a more concrete aim has been added recently: realization of a process proposed in a  $D - {}^3\text{He}$  fuelled FRC fusion reactor ARTEMIS-L<sup>[10]</sup>.

FRC plasma is of a long cylindrical shape and an extremely high- $\beta$  configuration which contains a purely poloidal magnetic field. In translation experiments, the FRC plasma is formed in a source region and launched into a confinement region. It goes along the magnetic field of the confinement region at a speed of the order of thermal velocity of the FRC source. The speed is usually more than 100 km/s. Subsequently, the FRC plasma hits against the magnetic mirror at the downstream end of the confinement region and reflected towards the magnetic mirror at the upstream end. It usually settles down with only a few times of reflection without severe degradation of confinement. That is, the rebound coefficient is considerably smaller than unity, being favorable for any purpose.

\*e-mail: takaku@uranus.phys.cst.nihon-u.ac.jp

†e-mail: hamada@helios.phys.cst.nihon-u.ac.jp

It had been reported that the rebound coefficients experimentally observed were consistent with MHD calculation for the FRX-C/T experiment at Los Alamos N. L. [5]. Since the classical ion mean free path ( $1.4 \sim 2.2m$ ) is less than the plasma length ( $\sim 4m$ ), it is natural for MHD to have been adequate for explanation of this experiment. However, it is not yet clear whether the rebound coefficient can be small or not for the plasma at translation stage in ARTEMIS, where the ion mean free path is to be several times the plasma length. It may be, therefore, worth to study such a simple model of reflection of collisionless FRC plasma as shown in Fig.1.

We consider a gas composed of neutral collisionless particles contained in a rigid cylindrical vessel with length  $l$  and cross-sectional area  $S$ . The mass of the vessel is assumed to be zero because it stands for the magnetic field inside the separatrix of FRC. The vessel initially moves with velocity  $u_0$  in  $\hat{x}$  direction toward a rigid wall which has infinite mass and is located at  $x = 0$ . The system hits upon the wall at a time  $t = 0$ , being reflected at a time  $t = t_1 (> 0)$  with velocity  $\bar{u}_1$  of center of mass. The particles are assumed to have at  $t = 0$  the Maxwellian velocity distribution of a temperature  $T_0$  (K) shifted by the velocity  $u_0$ .

In the next section, the rebound coefficient  $e = |\bar{u}_1|/u_0$  and the time  $t_1$  of contact with the rigid wall is exactly calculated as a function of  $U_0 = u_0/v_{th0}$  where  $v_{th0} = \sqrt{k_B T_0/m}$  with  $k_B$  the Boltzman constant and  $m$  the mass of each particle. In §3, quantities relevant to reflection are calculated and graphically shown to understand what take places during the time  $t_1$ .

The rebound coefficient takes the minimum value ( $\sim 0.365$ ) as  $U_0 \rightarrow 0$ , monotonically increases with  $U_0$  and tends to unity as  $U_0 \rightarrow \infty$ . Therefore, unless  $U_0 \gg 1$ , small rebound coefficients can be expected in case of long mean free path too. This feature of collisionless gas contrasts with that of collision dominated fluid. In §4, we briefly study for comparison a system of collision dominated fluid contained in a rigid vessel. As a result, the rebound coefficient is to be unity at slow injection ( $U_0 \rightarrow 0$ ) and decreases to  $\sim 0.5$  as  $U_0 \rightarrow \infty$ . In §5, the rebound coefficients are compared with two experiments, FIX (Osaka U.) and FRX-C/T (Los Alamos N.L.) and agreement is satisfactorily good for this simple model. In addition, the data of FIX exhibits the collisionless feature and the data of FRX-C/T the fluid-like one. Examination of classical ion mean free path supports this observation. §6 is conclusion.

## 2 Rebound Coefficient and Time of Contact

According to the assumption of our model explained in the last section, the particles in the cylindrical vessel are moving with the shifted Maxwellian distribution

$$f_0(v) = n_0 \sqrt{\frac{m}{2\pi k_B T_0}} \exp\left(-\frac{m(v - u_0)^2}{2k_B T_0}\right) \quad (1)$$

at the instant  $t = 0$  when the vessel hits against the wall. Here,  $v$  is the  $x$  component of the velocity of particle and  $n_0$  the number density of particles at  $t = 0$  assumed to be uniform in the vessel.

We make further assumptions that the particles are elastically reflected by the wall of the vessel and that the momentum and the kinetic energy of each particle in the  $x$  direction are not exchanged with the ones in the other directions. Consequently, the

kinetic temperature and velocity distribution in the other directions are unchanged in the process of reflection. As for the  $x$  component of the velocity of each particle, its absolute value  $|v(t)|$  can be considered as a virtual constant of motion as long as the vessel is in contact with the rigid wall at  $x = 0$  although, exactly speaking, it is not a constant of motion because it vanishes at the walls of the vessel.

Now, let us suppose for the moment that the vessel is fixed at rest for  $t \geq 0$ , and calculate the distribution function  $f(x, v, t)$  for  $t > 0$ . First, it can be confirmed that every particle for which  $x + (k+1)l > vt > x + kl$  at  $t$  ( $k = 0, \pm 1, \pm 2, \dots$ ) collides with either of the left or right wall of the vessel  $|k|$  times during the interval from 0 to  $t$ . Then, we have

$$\begin{aligned} f(x, v, t) &= f_0(v) \quad \text{for } x + (2k+1)l > vt > x + 2kl \quad -l < x < 0 \\ f(x, v, t) &= f_0(-v) \quad \text{for } x + 2kl > vt > x + (2k-1)l \quad -l < x < 0 \end{aligned} \quad (2)$$

because  $f(x(t), v(t), t)$  and  $|v(t)|$  are constants of motion. That is,  $f(x, v, t) = f_0(v)$  for  $(x, v)$  being in the white stripes of the phase space shown in Fig.2 and  $f(x, v, t) = f_0(-v)$  for  $(x, v)$  being in the shaded stripes. Exactly speaking, the distribution function can not be defined for  $x = -l, 0$  and  $vt = x + kl$ . Glancing at Fig.2, one can easily see that  $\lim_{x \rightarrow -l} f(x, v, t)$  and  $\lim_{x \rightarrow 0} f(x, v, t)$  are even functions of  $v$ , and then, the mean velocity of particles vanishes on the walls of the vessel.

Utilizing the distribution function just obtained, we calculate the force  $F(t)\hat{x}$  at  $t > 0$  exerted on the vessel by the contained particles. Note that this force is equal to the one exerted by the vessel on the wall at  $x = 0$  since the vessel has no mass.

$$\begin{aligned} F(t) &= Sm \left\{ \int_{-\infty}^{\infty} dv v^2 \lim_{x \rightarrow 0} f(x, v, t) - \int_{-\infty}^{\infty} dv v^2 \lim_{x \rightarrow -l} f(x, v, t) \right\} \\ &= 2Sm \sum_{k=-\infty}^{\infty} \left\{ \int_{\frac{2kl}{t}}^{\frac{(2k+1)l}{t}} dv v^2 f_0(v) - \int_{\frac{(2k-1)l}{t}}^{\frac{2kl}{t}} dv v^2 f_0(v) \right\} . \end{aligned} \quad (3)$$

Defining non-dimensional quantities as  $\Phi = F/n_0 k_B T_0 S$  and  $\tau = t v_{th0}/l$ , and using eq.(1), we have

$$\begin{aligned} \Phi(\tau, U_0) &= \sqrt{\frac{8}{\pi}} \sum_{k=-\infty}^{\infty} \left\{ \left[ (\xi + 2U_0) \exp\left(-\frac{\xi^2}{2}\right) \right]_{\frac{(2k-1)l}{\tau} - U_0}^{\frac{2k}{\tau} - U_0} - (1 + U_0^2) \int_{\frac{(2k-1)l}{\tau} - U_0}^{\frac{2k}{\tau} - U_0} d\xi \exp\left(-\frac{\xi^2}{2}\right) \right\} \\ &\quad + 2(1 + U_0^2) . \end{aligned} \quad (4)$$

As for limiting cases, we have

$$\lim_{\tau \rightarrow 0} \Phi(\tau, U_0) = \sqrt{\frac{8}{\pi}} \left\{ U_0 \exp\left(-\frac{U_0^2}{2}\right) + (1 + U_0^2) \int_{-U_0}^0 d\xi \exp\left(-\frac{\xi^2}{2}\right) \right\} \quad (5)$$

$$\lim_{\tau \rightarrow \infty} \Phi(\tau, U_0) = 0 . \quad (6)$$

In Fig.3,  $\Phi$  vs  $\tau$  are shown for values of  $U_0$  : (a) for  $U_0 = 1.0$  and (b) for  $U_0 = 5.0$ .

As it can be seen from the figures and eq.(5),  $\Phi$  is always positive for sufficiently small  $\tau$ . Let us denote by  $\tau_1$  the value of  $\tau$  at which  $\Phi$  vanishes for the first time. The vessel continues in contact with the wall during  $0 \leq \tau \leq \tau_1$  but lift off it just after  $\tau = \tau_1$  since a

negative force can not be exerted on the wall. So, we call  $t_1 = \tau_1 l/v_{th0}$  the time of contact or lift-off time.  $\tau_1$  is a function of  $U_0$  as shown in Fig.4. It decreases monotonically as  $U_0$  increases. From the figure, it seems to tend to zero as  $U_0 \rightarrow \infty$  and this conjecture will be confirmed mathematically later.

The rebound coefficient  $e$  is now calculated in the following way. Since the gas contained in the vessel has given the wall the momentum  $\int_0^{t_1} F(t)dt$ , it has gained the same amount of momentum with negative sign from the wall. Since it had initially the momentum  $S l n_0 m u_0$ , the total momentum at  $t = t_1$  is determined, and the velocity  $\bar{u}_1$  of the center of mass for  $t \geq t_1$  as well. So, we get

$$e = \frac{|\bar{u}_1|}{u_0} = \frac{\int_0^{t_1} F(t)dt - S l n_0 m u_0}{S l n_0 m u_0} = \frac{\int_0^{\tau_1} \Phi(\tau)d\tau - U_0}{U_0} . \quad (7)$$

In Fig.5, the coefficient  $e$  vs  $U_0$  is shown for the range  $0 < U_0 \leq 50$ . In Fig.9, it is shown for the narrow range  $0 < U_0 \leq 10$ . It takes the minimum value 0.365 as  $U_0 \rightarrow 0$ , and monotonically increases with  $U_0$ . From the figure, it seems to tend to unity as  $U_0 \rightarrow \infty$ . This can be confirmed mathematically by noticing that  $f_0(v)$  with a fixed  $u_0$  becomes close to  $n_0\delta(v - u_0)$  as  $v_{th0} \rightarrow 0$ , where  $\delta$  means Dirac's delta function. In this case,  $F$  is easily calculated to be equal to  $2S n_0 m u_0^2$  for  $0 < t < t_1 = l/u_0$ , and then,  $e$  is equal to unity. By the way, we have  $\tau_1 = t_1 v_{th0}/l = v_{th0}/u_0 = U_0^{-1}$ . Therefore, the conjecture from Fig.4 has been confirmed.

Now, let us consider the case of finite  $U_0$ . If we rewrite the definition of  $\tau_1$  as  $\tau_1 = v_{th0}/(l/t_1)$ ,  $\tau_1$  gets a new meaning: the ratio of the width  $v_{th0}$  of the initial distribution function  $f_0(v)$  to the vertical width of the stripes in Fig.2 at  $t = t_1$ . Note that this ratio decreases from  $\sim 0.55$  to 0 as  $U_0$  increases from 0 to  $\infty$ . Similarly, if we rewrite  $\tau_1 U_0$  as  $\tau_1 U_0 = u_0/(l/t_1)$ ,  $\tau_1 U_0$  gets a meaning: the vertical position of the center of symmetry of  $f_0(v)$  in the phase space normalized by the vertical width of the stripes at  $t = t_1$ . From Fig.4, it can be confirmed that  $\tau_1 U_0$  the relative position of the center of symmetry of  $f_0(v)$  change from 0 to unity as  $U_0$  increases from 0 to  $\infty$ . From these observations, it can be seen that the smaller  $U_0$  is, the more symmetric  $f(x, v, t_1)$  is with respect to  $v$ . Therefore, the smaller  $U_0$  is, the smaller the rebound coefficient  $e = |\bar{u}_1|/u_0$  is, where  $\bar{u}_1 = \int v f(x, v, t_1) dv dx / n_0 l$ .

According to the Boltzmann's H theorem, the entropy of our system of collisionless gas does not change in the process of reflection. So, it may be necessary to explain why the coefficient  $e$  could be less than unity for the system without dissipation. When  $e < 1$ , a part of the incident kinetic energy is temporarily transformed into a free energy associated with the deviation from the Maxwellian distribution. After a long while, it may eventually be dissipated into thermal energy by rare collisions between particles.

### 3 Quantities Relevant to Reflection

With use of the distribution function obtained in the last section, some quantities relevant to reflection are calculated and shown in graphs here. The number density of particles  $n(x, t)$  defined as

$$n(x, t) = \int_{-\infty}^{\infty} dv f(x, v, t)$$

can be written as  $n = n_0 N(X, \tau; U_0)$  where  $X = x/l$  and

$$N(X, \tau; U_0) = \frac{1}{\sqrt{2\pi}} \sum_{k=-\infty}^{\infty} \left\{ \int_{\frac{X+2k}{\tau}-U_0}^{\frac{X+2k+1}{\tau}-U_0} d\xi \exp\left(-\frac{1}{2}\xi^2\right) + \int_{\frac{X+2k-1}{\tau}+U_0}^{\frac{X+2k}{\tau}+U_0} d\xi \exp\left(-\frac{1}{2}\xi^2\right) \right\}. \quad (8)$$

It can be shown that  $N(X, 0) = N(X, \infty) = N(-\frac{1}{2}, \tau) = 1$  and that  $N(X, \tau) + N(-1 - X, \tau) = 2$ :  $N - 1$  is an odd function of  $X + 1/2$ . This function is shown in Fig.6 for  $U_0 = 5.0$ .<sup>1</sup>

The average velocity of particles  $u(x, t)$  defined as

$$u(x, t) = \frac{1}{n(x, t)} \int_{-\infty}^{\infty} dv v f(x, v, t)$$

can be written as  $u = v_{th0} U(X, \tau; U_0)$  where

$$U(X, \tau; U_0) = \frac{1}{N\sqrt{2\pi}} \sum_{k=-\infty}^{\infty} \left\{ \int_{\frac{X+2k}{\tau}-U_0}^{\frac{X+2k+1}{\tau}-U_0} d\xi (\xi + U_0) \exp\left(-\frac{1}{2}\xi^2\right) + \int_{\frac{X+2k-1}{\tau}+U_0}^{\frac{X+2k}{\tau}+U_0} d\xi (\xi - U_0) \exp\left(-\frac{1}{2}\xi^2\right) \right\} \quad (9)$$

It can be shown that  $\lim_{X \rightarrow 0} U(X, \tau) = 0$  and  $\lim_{X \rightarrow -1} U(X, \tau) = 0$  and that  $N(X, \tau)U(X, \tau)$  is an even function of  $X + 1/2$ . It can also be shown that  $\lim_{\tau \rightarrow 0} U(X, \tau) = U_0$  for  $-l < x < 0$  and  $\lim_{\tau \rightarrow \infty} U(X, \tau) = 0$  for  $-l \leq x \leq 0$ . This function is shown in Fig.7 for  $U_0 = 5.0$ .

The kinetic temperature  $T(x, t)$  in the  $x$  direction defined as

$$T(x, t) = \frac{m}{k_B n(x, t)} \int_{-\infty}^{\infty} dv \{v - u(x, t)\}^2 f(x, v, t)$$

can be written as  $T = T_0 \Theta(X, \tau; U_0)$  where

$$\Theta(X, \tau; U_0) = \frac{1}{N\sqrt{2\pi}} \sum_{k=-\infty}^{\infty} \left\{ \int_{\frac{X+2k}{\tau}-U_0}^{\frac{X+2k+1}{\tau}-U_0} d\xi (\xi + U_0 - U)^2 \exp\left(-\frac{\xi^2}{2}\right) + \int_{\frac{X+2k-1}{\tau}+U_0}^{\frac{X+2k}{\tau}+U_0} d\xi (\xi - U_0 - U)^2 \exp\left(-\frac{\xi^2}{2}\right) \right\}. \quad (10)$$

This function is shown in Fig.8 for  $U_0 = 5$ .

Finally, the pressure tensor is diagonal. Two diagonal elements corresponding to the directions perpendicular to the  $x$  axis are equal to  $k_B T_0 n(x, t)$  and the element corresponding to the  $x$  direction is equal to  $k_B T(x, t) n(x, t)$ .

## 4 Brief study of collision dominated fluid

For comparison, we briefly study the rebound coefficient  $e$  of the system with collision dominated fluid instead of collisionless gas. We will consider only two extreme cases that  $U_0 \rightarrow 0$  and that  $U_0 \rightarrow \infty$ .

<sup>1</sup>Of course, eqs.(8),(9) and (10) do not hold for  $\tau > \tau_1$  unless the vessel is kept at rest on the wall.

When the  $x$  component  $u$  of the fluid velocity is very small compared with the sound velocity  $C_{s0}$  at  $t = 0$ ,  $u$  is subject to the D'Alembert's equation

$$\frac{\partial^2 u}{\partial x^2} - \frac{1}{C_{s0}^2} \frac{\partial^2 u}{\partial t^2} = 0$$

where viscosity has been neglected since the viscosity coefficient is proportional to collision time between particles<sup>[13]</sup>. Our problem of reflection is reduced to the initial and boundary value problem with conditions

$$\begin{aligned} u(x, 0) &= u_0 & \text{for } -l < x < 0 \\ u(-l, t) &= u(0, t) = 0 & \text{for } t > 0 \end{aligned} \quad (11)$$

From the solution, it is seen that  $u(x, t_1) = -u_0$  for  $-l < x < 0$  where  $t_1 = l/C_{s0}$ . The velocity of the vessel after reflection, therefore, is equal to  $-u_0$  and then  $e = 1$ .

Next, let us consider the case that the incident mach number  $M_0$  is much greater than unity, where  $M_0 = u_0/C_{s0} = U_0/\sqrt{\gamma}$  with  $\gamma$  the ratio of specific heats. A uniform flow with velocity  $u_0$  and pressure  $p_0 = n_0 k_B T_0$  is formed in the vessel at  $t = 0$ . The upstream end of it becomes a rarefaction wave the tail of which continues to the vacuum region. The width of the rarefaction wave is equal to  $C_{s0} t (\gamma + 1) / (\gamma - 1)$ , so that the upstream end of the uniform flow can be considered as being sharp cut when  $M_0 \gg 1$ . The downstream end of the uniform flow is a front of shock wave. The fluid between the shock front and the right wall of the vessel is at rest and of pressure  $p_0 \gamma (\gamma + 1) M_0^2 / 2$ . The velocity of the shock front is equal to  $-(\gamma - 1)u_0/2$ , so that the shock front reaches at  $t = 2l / \{(\gamma + 1)u_0\}$  the upstream end of the uniform flow at  $x = -l(\gamma - 1) / (\gamma + 1)$ .

Then, a rarefaction wave spreads from there, and its left and right fronts reach the left and right walls of the vessel at the same time  $t = t'$  where

$$t' = \frac{2l}{(\gamma + 1)u_0} \left( 1 + \sqrt{\frac{\gamma - 1}{2\gamma}} \right) \quad (12)$$

A new shock wave, then, emerges at the left wall, where the pressure increases and reaches the one at the right wall at  $t = t_1$  the lift-off time. We, therefore, obtain a lower bound of the rebound coefficient  $e$  :

$$e > \sqrt{\frac{\gamma - 1}{2\gamma}} = 0.447 \quad \text{for } \gamma = \frac{5}{3} \quad (13)$$

using  $t'$  instead of  $t_1$  in eq.(8).

An upper bound of  $e$  is obtained by assuming that all the work done by adiabatic expansion of the fluid from the volume  $Sl(\gamma - 1) / (\gamma + 1)$  to the full volume  $Sl$  is transformed into the kinetic energy of translation after reflection. That is, we have

$$e < \sqrt{1 - \left( \frac{\gamma - 1}{\gamma + 1} \right)^{\gamma - 1}} = 0.777 \quad \text{for } \gamma = \frac{5}{3} \quad (14)$$

Any way, the rebound coefficient of collision dominated fluid decreases as the incident parameter  $U_0$  increases. This is a tendency reverse to the one of collisionless gas.

## 5 Comparison with Experiments

In Fig.9, rebound coefficient vs  $U_0$ 's estimated by us from papers of two experiments are plotted together with the curve calculated in §2. The circles have been marked on the basis of FRX-C/T experiment at Los Alamos<sup>[5]</sup> and the squares on the basis of FIX experiment at Osaka<sup>[8]</sup>. It, however, was necessary apriori to assume that the ion temperature  $T_i$  is equal to the electron temperature  $T_e$  because these papers provide only the total temperature  $T_i + T_e$ . Except for this assumption, The black circle has been plotted with direct use of Figs.5, 6 and 7(a) in ref. 5, and the black square with direct use of Figs. 5, 7 and 9 in ref. 8. For the other marks, rather indirect methods were necessary. For the white circle, the total temperature was estimated from the datum on table I, eq.(3) and the average value of  $v_z$  for  $B_0 = 4.5kG$  on Fig.5 in ref.5. Here,  $v_z$  is the velocity of translation corresponding to our  $u_0$ , and  $B_0$  means the magnetic field in the confinement region in absence of plasma. The two white squares have been plotted with use of the average data for the highest and the lowest value of  $B_0$  on Figs. 5 and 7 in ref.8, which were assumed to correspond to the averaged data of first transit in Fig. 11 for the highest temperature and the lowest one, respectively.

Agreement between experiments and calculation is satisfactorily good for simplicity of our model. Furthermore, it can be seen from the figure that the rebound coefficients observed in FRX-C/T are greater than the calculated ones and their dependence on  $U_0$  is reverse to the curve calculated for the collisionless gas but has the similar dependence as that of the collision dominated fluid. The ion classical collision mean free paths<sup>[11]</sup> for FRX-C/T are estimated to be  $1.4 \sim 2.2m$ , which are slightly shorter than the plasma length ( $\sim 4m$ ). Thus, the fluid-like character suggested by the dependence of the rebound coefficient on the incident speed has been supported by estimation of the ion collision mean free path.

As for FIX experiment, it can be seen that the rebound coefficients observed are less than the calculated ones and their dependence on  $U_0$  is similar to the curve calculated for the collisionless gas. In this case, estimation of the ion mean free path is not unique on account of abrupt increase of the total temperature  $T_i + T_e$  at the time of reflection. This phenomenon was explained as rethermalization by formation of a shock wave<sup>[8]</sup>. In fact, the incident Mach's numbers were greater than unity in this experiment. If we use the temperature just before reflection, the ion mean free paths are estimated to be only  $0.08 \sim 0.41m$ , being much shorter than the plasma length  $\sim 4m$ . If we use the temperature just after reflection and assume that only the ions are heated by shock formation, the ion mean free paths are estimated to be  $2 \sim 6m$  and comparable with the plasma length. These estimation of the mean free paths, however, is not suitable for examining adequacy of our collisionless gas model. Since the Mach's number is greater than unity, particles reflected at the rigid wall should be regarded as the "test particles" with velocity  $2u_0$  incident into the "field plasma"<sup>[12]</sup> with the temperature before reflection. Then, the ion mean free path are estimated to be  $4.3 \sim 15.6m$  and longer than the plasma length<sup>2</sup>. Thus, in this case too, the collisionless character suggested by the dependence of the rebound coefficients on the incident speed has been supported by estimation of the ion collision mean free path.

The rebound coefficients observed in FIX experiment are smaller than calculated ones.

<sup>2</sup>In order to obtain these values, we multiplied  $2u_0$  by the smaller value of the slowing-down time and the deflection time, taking account of both ions and electrons in the field plasma.

This may be due to the fact that the magnetic field in the confinement region is very weak ( $100 \sim 700G$ ) compared with that of FRX-C/T experiment ( $2 \sim 4.5kG$ ) while the magnetic field in the source region (1T) is comparable to that of FRX-C/T(0.6T).

## 6 Conclusion

We have proposed a very simple model of reflection of field-reversed configuration and calculated its rebound coefficient together with the relevant quantities. It takes the minimum value ( $\sim 0.365$ ) at slow incident speed and increases up to unity as  $U_0 \rightarrow \infty$ . As a result, rebound coefficients considerably smaller than unity can be expected for future collisionless FRC's unless  $U_0 \gg 1$ . A fluid-like model has also been briefly studied and shown that it has opposite tendency from our collisionless model. The calculation has been compared with two experiments. Agreement is satisfactorily good for simplicity of our model. In addition, by examining dependence of the rebound coefficient on the incident speed, we have been able to make a successful conjecture on whether the ion mean free paths is longer or shorter than the plasma length. This gives us expectation of diagnostic use of reflection experiment of FRC.



## References

- [1] A.G.Es'kov, R.Kh.Kurtmullaev, A.P.Kreshchuk, et al., in *plasma Physics and Controlled Nuclear Fusion Research 1978 (Proc. 7th Int. Conf. Innsbruck, 1978)*, Vol. 2, IAEA, Vienna (1979) 187.
- [2] W.T. Armstrong, R.K.Linford, J.Lipson, D.A.Platts, E.G.Sherwood, *Phys. Fluids* **24** (1981) 2068.
- [3] T.Minato, M.Tanjyo, S.Okada, Y.Ito, M.Kako, S.Ohi, S.Goto, T.Ishimura, H.Ito, in *Proceedings of the Japan-US Joint Workshop on Compact Toroids (Osaka, 1982)*, Osaka University (1982) 191.
- [4] M.Tanjyo, S.Okada, Y.Ito, M.Kako, S.Ohi, S.Goto, T.Ishimura, H.Ito, Y. Nogi, S.Shimamura, T.Ikama, S.Hamada, in *Plasma Physics and Controlled Nuclear Fusion Research 1984 (Proc. 10th Int. Conf. London, 1984)*, Vol. 2, IAEA, Vienna (1985) 523
- [5] D.J. Rei, W.T.Armstrong, R.E.Chrien, P.L.Klingner, R.K.Linford, K.F.McKenna, E.G.Sherwood, R.E.Siemon, M.Tuszewski, *Phys. Fluids* **29** (1986) 852.
- [6] M.Tuszewski, W.T.Armstrong, R.E.Chrien, P.L.Klingner, K.F.McKenna, D.J.Rei, E.G.Sherwood, R.E.Siemon, *Phys. Fluids* **29** (1986) 863.
- [7] Wang G., Wang S., Chang Q., *Nucl. Fusion Plasma Phys.(China)* **7** (1987) 202.
- [8] H.Himura, S.Okada, S.Sugimoto, S. Goto, *Phys. Plasmas*, Vol. 2, (1995) 191
- [9] M.Tuszewski, *Nuclear Fusion* **28** (1988) 2033.
- [10] H.Momota, Y.Tomita, A.Ishida, Y.Kohzaki, Y.Nakano, M.Nishikawa, Sh.Ohi, M.Ohnishi, in *Plasma Physics and Controlled Nuclear Fusion Research 1992 (Proc. 14th Int. Conf. Wurzburg, 1992)*, Vol. 3, IAEA, Vienna (1993) 319
- [11] L.Spitzer, Jr., *Physics of Fully Ionized Gases*, 2nd ed. (Wiley, New York 1962).
- [12] B.A.Trubnikov, *Review of Plasma Physics* edited by M.A.Leontovich (Consultants Bureau, New York 1965) Vol. 1 p105.
- [13] S.I. Braginskii, *Review of Plasma Physics* edited by M.A.Leontovich (Consultants Bureau, New York 1965) Vol. 1 p205.

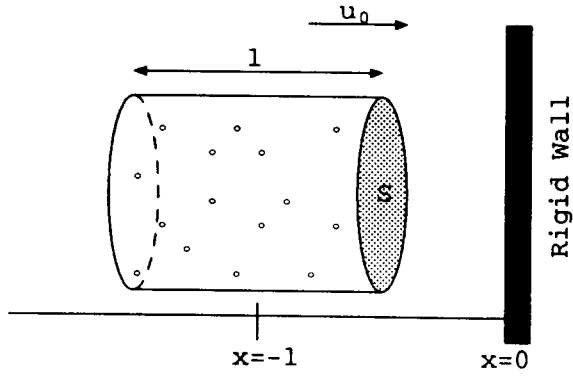


Fig. 1. A model of collisionless FRC reflected by a magnetic mirror. A rigid cylindrical vessel without mass and a rigid wall at  $x = 0$  stand for the magnetic field of FRC and the magnetic mirror, respectively. The cylinder contains a neutral collisionless gas instead of a plasma and hits upon the wall with a velocity  $u_0$  at time  $t = 0$ .

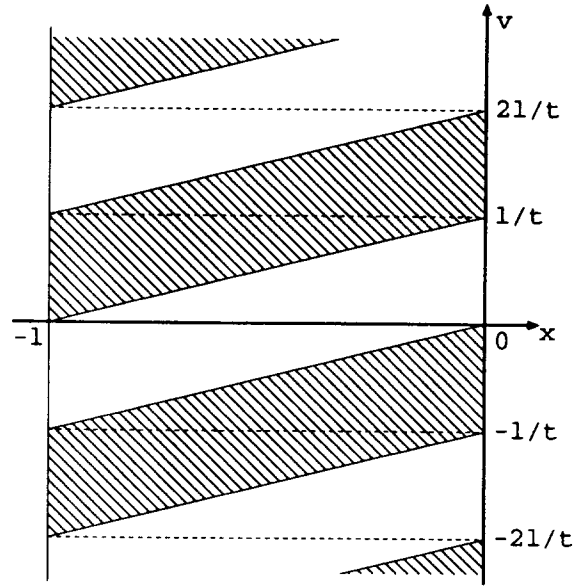


Fig. 2. The phase space of single particle at  $t > 0$ . The distribution function  $f(x, v, t)$  of particles in the vessel at rest on the wall is equal to  $f_0(v)$  for the point in the white stripes and equal to  $f_0(-v)$  for the point in the shaded ones.  $f_0$  is the distribution at  $t = 0$  and  $l$  the length of the vessel.

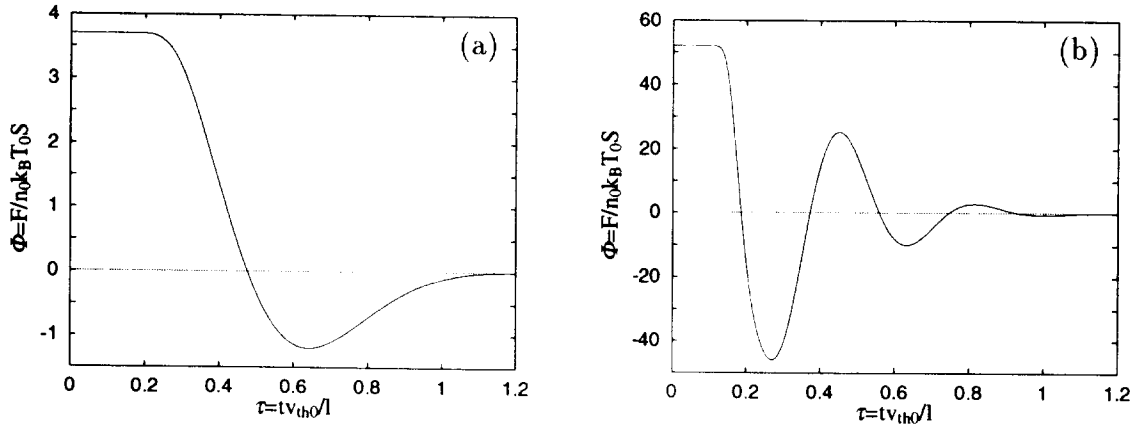


Fig. 3. The force  $F(t)$  at time  $t > 0$  exerted on the wall by the system fixed on it, (a) for  $U_0 = 1$  and (b) for  $U_0 = 5$ .  $U_0$  is the incident velocity  $u_0$  normalized by the thermal velocity  $v_{th0} = \sqrt{k_B T_0 / m}$ .  $S$  and  $l$  are the cross-sectional area and the length of the vessel, respectively.  $n_0$  is the number density of particles. The suffix 0 means values of  $t = 0$ .

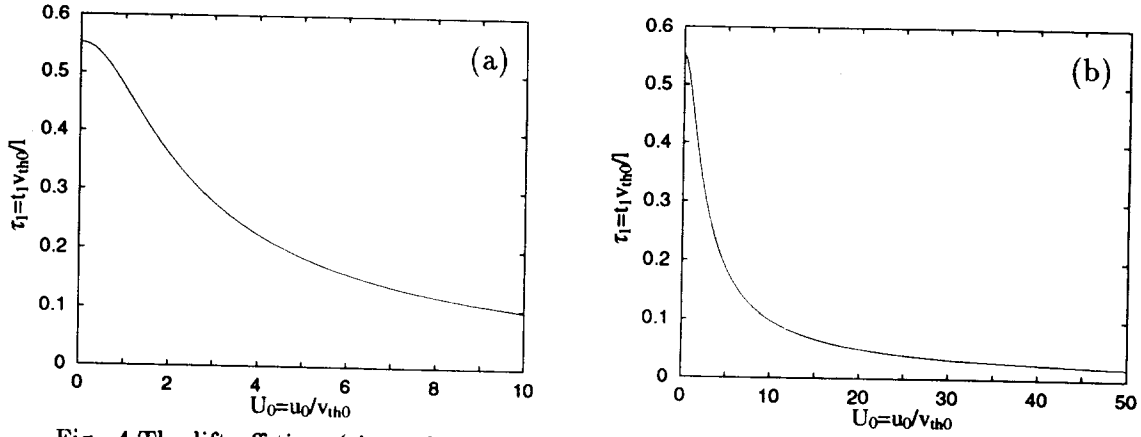


Fig. 4. The lift-off time (time of contact)  $t_1$  of the system from the wall, (a) for the range  $0 < U_0 < 10$  and (b) for the range  $0 < U_0 < 50$ .  $t_1$  is obtained as the first zero of the force  $F(t)$ . See Fig. 3.

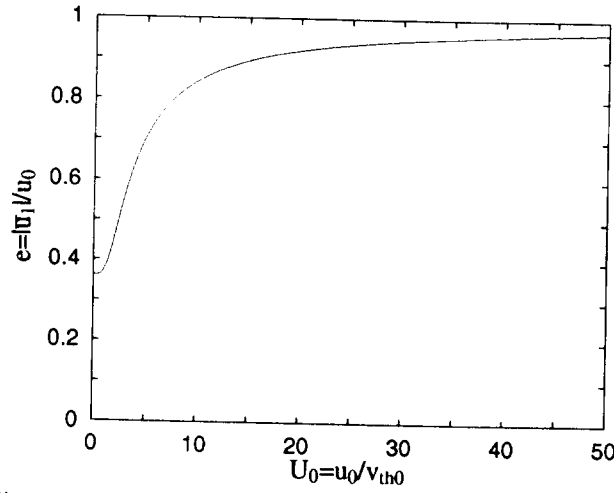


Fig. 5. The rebound coefficient  $e$  vs  $U_0$ . It tends to unity as  $U_0 \rightarrow \infty$ .  $\bar{u}_1$  is the velocity of the center of mass at the lift-off time  $t_1$ .

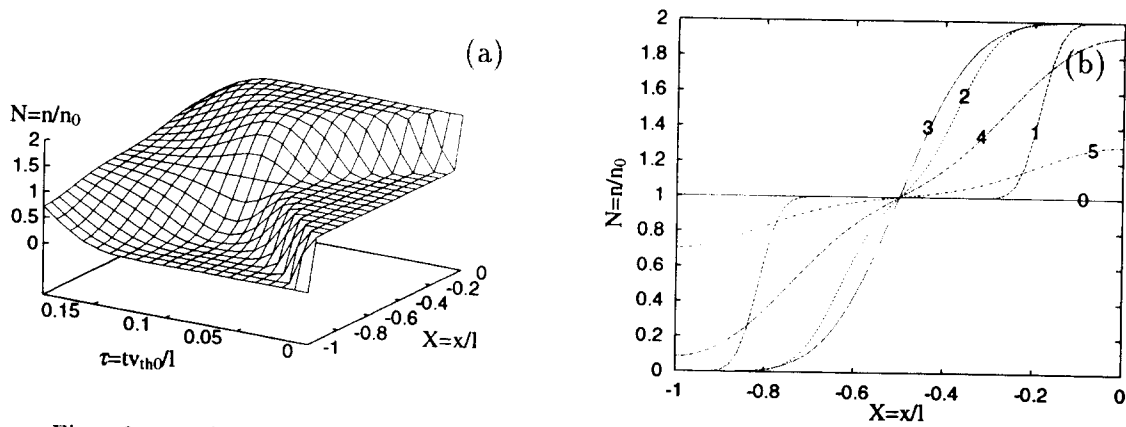


Fig. 6. Evolution of the number density  $n$  of particles during the time of contact for  $U_0 = 5.0$ . In this case,  $\tau_1 = 0.186$ . (a) three dimensional view and (b) the curve numbered  $n$  ( $0 \sim 5$ ) corresponds to the time  $\tau = (n/5)\tau_1$

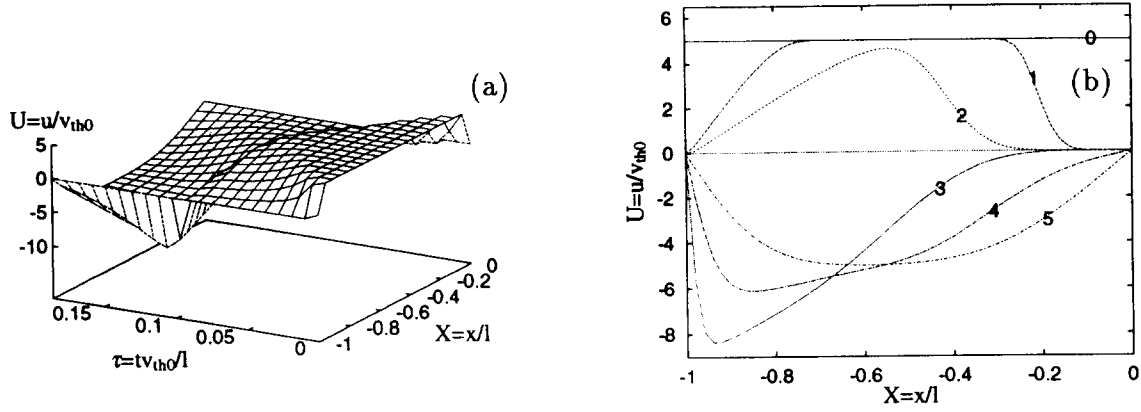


Fig. 7. Evolution of the average velocity  $u$  of particles during the time of contact for  $U_0 = 5.0$ . In this case,  $\tau_1 = 0.186$ . (a) three dimensional view and (b) the curve numbered  $n$  ( $0 \sim 5$ ) corresponds to the time  $\tau = (n/5)\tau_1$

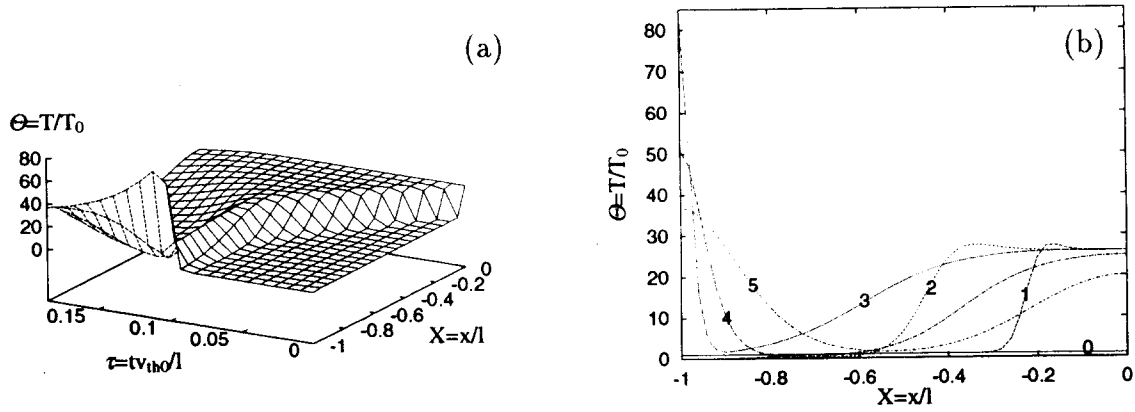


Fig. 8. Evolution of the kinetic temperature  $T$  in  $x$  direction during the time of contact for  $U_0 = 5.0$ . In this case,  $\tau_1 = 0.186$ . (a) three dimensional view and (b) the curve numbered  $n$  ( $0 \sim 5$ ) corresponds to the time  $\tau = (n/5)\tau_1$

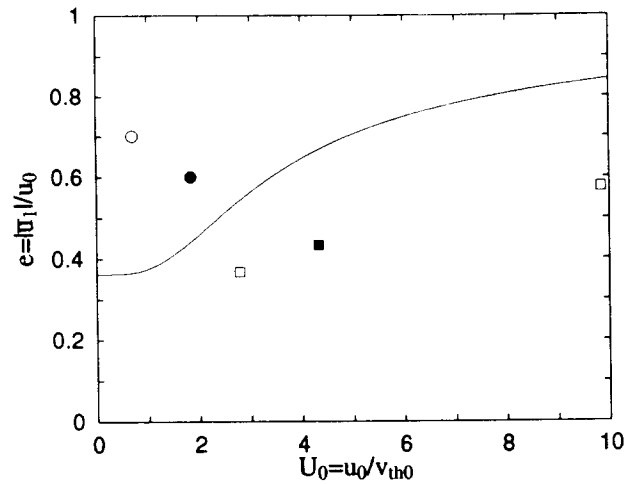


Fig. 9. Comparison of the rebound coefficient  $e$  calculated on the basis of our model with those observed in FIX experiment at Osaka U. (squares) and those in FRX-C/T experiment at Los Alamos N.L. (circles). See the text for difference between black marks and white ones.